

Original Article

CircUBR5 acts as a ceRNA for miR-1179 to up-regulate UBR5 and to promote malignancy of triple-negative breast cancer

Guohua Gong^{1,2}, Jikai She^{2,3}, Danni Fu^{2,3}, Dong Zhen^{2,3}, Bin Zhang^{1,2}

¹First Clinical Medical of Inner Mongolia Minzu University, Tongliao, Inner Mongolia, P. R. China; ²Inner Mongolia Key Laboratory of Mongolian Medicine Pharmacology for Cardio-Cerebral Vascular System, Tongliao, Inner Mongolia, P. R. China; ³Medicinal Chemistry and Pharmacology Institute, Inner Mongolia Minzu University, Tongliao, Inner Mongolia, P. R. China

Received November 9, 2021; Accepted May 11, 2022; Epub June 15, 2022; Published June 30, 2022

Abstract: UBR5 is an E3 ubiquitin ligase and an oncogene in a panel of human cancers. However, little is known on its impacts in triple-negative breast cancer (TNBC) and even less on its relationship to circUBR5 (hsa_circ_0001819), a circular RNA derived from exons 2, 3, 4, and 5 of UBR5 gene. In this study, we detected higher expressions of both circUBR5 and UBR5 in TNBC tissues, which were associated with worse prognosis, and also in a panel of breast cancer cells, particularly in TNBC cells. Functionally, circUBR5 was crucial for sustaining the malignant growth and metastasis of TNBC cells both *in vitro* and *in vivo*. Mechanistically, the oncogenic phenotypes of circUBR5 were mediated through sponging miR-1179 and up-regulating UBR5. Concomitant silencing circUBR5 and miR-1179 abolished the anti-tumor effects of targeting circUBR5 alone. Therefore, targeting circUBR5/miR-1179/UBR5 axis may benefit the treatment of TNBCs.

Keywords: Triple-negative breast cancer, circUBR5, miR-1179, UBR5, miRNA sponge

Introduction

Triple-negative breast cancer (TNBC), featuring absent expressions of estrogen, progesterone, and Her2 receptors, comprises approximately 10-15% of all breast cancer cases [1]. Among different breast cancer subtypes, TNBC represents the most malignant subtype, associated with aggressive metastasis, early relapse, and poor prognosis. Despite the availability of therapeutic strategies including surgery, radiotherapy, and chemotherapy, the current treatment for TNBC remains unsatisfactory, mainly due to the lack of effective drug targets [2]. Therefore, identifying molecules critically regulating the pathogenesis of TNBC will help to reveal novel diagnostic or prognostic biomarkers and develop potential therapies.

In recent years, accumulating evidence has revealed the importance of circular RNAs (circRNAs) in cancer development and progression [3]. Derived from exons and/or introns of par-

ent genes that normally also produce linear isoforms, circRNAs are generally highly conserved across species and carry a loop structure without free ends. Consequently, circRNAs usually present superb structural stability and may act via multiple mechanisms in different subcellular compartments, including nucleus, cytoplasm, as well as exosomes [4]. A most common mechanism for circRNAs is by acting as the competitive endogenous RNAs (ceRNAs) to sequester or sponge miRNAs from their target mRNAs, thereby regulating various pathological processes [5-8]. Besides, circRNAs may also regulate the expression of their parent genes, although the functional significance of such regulation has not been extensively explored [9]. To date, the research on circRNAs in TNBC is still in its infancy, with less than 35 studies published by far.

The E3 ubiquitin ligase UBR5 is overexpressed in a panel of human cancers and associated with poor patient prognosis [10-13]. In TNBC,

however, only one study has reported that UBR5 gene is amplified and essentially drives the growth, metastasis, angiogenesis, and epithelial-mesenchymal transition (EMT) of TNBC cells, supporting its value as a therapeutic target [14]. To further characterize the significance of UBR5 in TNBC, to explore other mechanisms that may lead to UBR5 up-regulation, and to understand the crosstalk between a circRNA and its parent gene in a disease paradigm, here we examine whether a circRNA derived from exons 2, 3, 4, and 5 of UBR5 gene, circUBR5 (hsa_circ_0001819), regulates UBR5 expression in TNBC, and if so, what underlying mechanisms are involved.

The innovative findings from this study are on several levels. First, it corroborates the oncogenic role of UBR5 in TNBC; second, by examining the regulation between circUBR5 and UBR5, it reveals a novel mechanism by which circUBR5 controls its parent gene and promotes the malignancy of TNBC; third, it provides preclinical evidence that targeting circUBR5 may benefit the management of TNBC. Therefore, this study suggests novel therapeutic strategies for TNBC.

Materials and methods

Declaration of ethics and collection of human samples

Experiments involving human samples and experimental animals were designed following the guidelines of and approved by the Research Ethics Committee of Inner Mongolia University for the Nationalities (Inner Mongolia, China). Fifty TNBC patients with a median age of 48 years receiving surgical excision were recruited into this study. Inclusion criteria: female aged 20-80 years old; did not receive any treatment related to breast cancer before admission; improved relevant examination after admission, unilateral primary breast cancer was diagnosed for the first time and no bone, lung, liver, brain metastasis or other metastasis was found by CT, bone scan, B-ultrasound and other imaging examination; postoperative pathology after puncture or minimally invasive breast biopsy; invasive breast cancer; breast cancer after breast conserving or modified radical mastectomy. The postoperative survival time was more than 6 months, and 6-8 cycles of neoadjuvant chemotherapy or adjuvant chemotherapy were performed.

Exclusion criteria: history of bilateral or pre-hospital breast cancer; breast cancer during pregnancy or lactation; intraductal carcinoma or lobular carcinoma in situ; bone, lung, liver, brain metastasis or other metastasis when diagnosed breast cancer; present or previous suffering from other malignant tumors; complicated with coronary heart disease, hypertension, cerebrovascular disease and other serious systemic diseases; patients with mental and neurological diseases unable to cooperate with treatment. The clinicopathological data were incomplete. A written consent was signed by each participant. Paired tumor and adjacent non-tumor (ANT) breast tissues were acquired during surgery and confirmed by pathological examinations. All dissected breast tissues were partially frozen in liquid nitrogen and partially fixed in formalin and prepared into paraffin sections till further analysis. All patients were followed up for 150 months (from August 2007 to March 2020) after the surgery.

Cell culture and transfection

The non-tumorigenic breast epithelial cell line MCF10A, non-TNBC cell lines (MCF-7 and SKBR-3), and TNBC cell lines (BT549, MDA-MB-231, and MDA-MB-468) were ordered from ATCC (Manassas, VA, USA). MCF10A cells were cultured in DMEM/F12 medium supplemented with 5% horse serum, 0.5 mg/mL hydrocortisone, 10 µg/mL insulin, 100 ng/mL cholera toxin, 20 ng/mL epidermal growth factor, and 1× penicillin/streptomycin. All breast cancer cells were cultured in RPMI1640 medium with 10% fetal bovine serum (FBS) and 1× penicillin/streptomycin. Reagents used for cell culture were purchased from Invitrogen (Carlsbad, CA, USA).

Two different siRNAs specifically targeting circUBR5 (si-circUBR5 #1: 5'-UAUCACUUUCUGU-UUCAGCUG-3'; and #2: 5'-UACUUUCACUAUC-ACUUUCUG-3', 50 nM for each) and the non-targeting control siRNA (si-NC) were custom designed by GenePharma (Shanghai, China). MiR-1179 mimics (miR-1179), control mimics (miR-NC), miR-1179 inhibitor (LNA-miR-1179), and control inhibitor (LNA-NC) were ordered from Qiagen (Valencia, CA, USA). Sequence of oligonucleotides used in this study, MiR-1179 mimics (miR-1179): 5'-AAGCAUUCUUUCAUUG-GUUGG-3', control mimics (miR-NC): 5'-UCA-CAACCUCCUAGAAAGAGUAGA-3'; miR-1179 inhibitor (LNA-miR-1179): 5'-5'-CCAACCAAUGA-

The circUBR5/miR-1179/UBR5 axis in TNBC

Table 1. Sequences of primers used for RT-PCR

Gene	Forward (5'-3')	Reverse (5'-3')
circUBR5	GTAGGACAAGCGACTCTCCA	TCCTCAAGAAGAAAGGCAGC
UBR5	CGTGTCTACAGGACTGGAATGC	AACAGTCCAGCCGAATTGTGCC
miR-1179	AGCATTCTTTCATTGGTTG	GAACATGTCTGCGTATCTC
GAPDH	GTCTCCTCTGACTTCAACAGCG	ACCACCCTGTTGCTGTAGCCAA
U6	CTCGCTTCGGCAGCACAT	TTTGCCTGTCATCCTTGGC
18S	ACCCGTTGAACCCATTCTGTA	GCCTACTAAACCATCCAATCGG

AAGAAUGCUU-3', control inhibitor (LNA-NC): 5'-UCUACUCUUUCUAGGAGGUUGUGA-3'. Transfection of siRNA, miRNA mimics, or miRNA inhibitor was performed following the instructions of Lipofectamine RNAiMAX (Invitrogen).

We used stable cells for *in vivo* assays. Lentivirus expressing the non-targeting control shRNA (sh-NC) and sh-circUBR5 (a mixture of two distinct sh-circUBR5). #1: 5'-CACCGCAACC-AAGATAATGCTAGTGCGAACACTAGCATTATCTTG-GTTGC-3'; #2: 5'-ACCGTTGCTGCGAGTACAAC-GCTTCAACGGAAGCGTTGTCAGTGCAGCAA-3', sh-NC: 5'-UUCUCCGAACGUGUCACGUUU-3'. (1 µg for each) together with puromycin selection gene, and that expressing miR-NC inhibitor and miR-1179 inhibitor together with neomycin selection gene were custom produced by Genomeditech (Shanghai, China) and transduced into MDA-MB-231 cells in the presence of polybrene (Solarbio, Beijing China). Stable cells were obtained by culturing the lentivirus-transduced cells in puromycin (3.5 µg/mL) and/or G418 (400 µg/mL, Solarbio) for 10 more days.

RNA stability and real-time PCR (RT-PCR)

For RNase R treatment, total RNA was extracted from MDA-MB-231 cells with Trizol (Invitrogen) and then treated with RNase R (10 U; BioVision, Mountain View, CA, USA) at 37°C for 30 min. To measure the RNA stability, MDA-MB-231 cells were treated with actinomycin D (2.5 µg/mL; Sigma, St. Louis, MO, USA) to block *de novo* gene transcription for 0, 4, 8, 12, and 24 h, respectively, before total RNA was extracted. RNA fractionation was performed using RNA Subcellular Isolation Kit (Active Motif, Carlsbad, CA, USA). Reverse transcription was performed using PrimeScript RT Reagent Kit (Takara, Dalian, China) and qPCR using SYBR Premix Ex Taq II Kit (Takara). Quality primers for RT-PCR analysis (Table 1) were synthesized by GeneChem (Shanghai, China). Relative gene

expression was analyzed using $2^{-\Delta\Delta Ct}$ method and normalized to U6 (for circRNAs or miRNAs) or GAPDH (for mRNAs).

Fluorescence *in situ* hybridization (FISH)

FITC-labeled RNA FISH probe detecting human circUBR5 was custom produced by Biosearch

Technologies (Shanghai, China) and FISH assay was performed on MDA-MB-231 cells following the instructions from Stellaris FISH Kit (Biosearch Technologies). Cell nuclei were stained with DAPI, and images were taken under a fluorescence microscope (Olympus IX-51, Tokyo, Japan).

Cell viability and proliferation assays

Cell Counting Kit-8 (Beyotime, Jiangsu, China) was used to measure cell viability. To measure the long-term proliferation of TNBC cells, target BT549 or MDA-MB-231 cells were seeded in triplicate at 200 cells/well into 24-well plates and cultured at 37°C for 10 days. The formed cell colonies were stained with 1% crystal violet. For short-term proliferation, Click-iT EdU Alexa Fluor 488 Imaging Kit (Thermo Fisher, Waltham, MA, USA) was used following the manufacturers' instructions. Cell nuclei were stained with DAPI. Cell images were taken under an Olympus IX-51 microscope.

Transwell invasion assay

Target cells resuspended in serum-free medium were seeded into the Matrigel-coated Transwell insert (8.0 µm; Corning, Lowell, MA, USA). Serum-containing medium was added to the lower chamber. After 24 h, we used cotton swabs to clear non-invading cells from the top of the insert membrane and stained the invading cells with 1% crystal violet. The invading cells were counted and photographed under an Olympus IX-51 microscope.

Migration assay

Wound healing was performed as described earlier to assess cell migration [15]. In brief, a scratch was made with a pipette tip across the confluent layer of target cells. Immediately (0 h) and after 24 h, respectively, pictures were taken of the scratch at an identical location and

the width (W) of the scratch was measured. The percentage (%) wound closure was determined as $(W_{0h} - W_{24h}) / W_{0h} \times 100\%$.

In vivo xenograft growth and experimental metastasis

Six-week-old female BALB/c nude mice were ordered from Shanghai SLAC Laboratory Animal Co. (Shanghai, China) and housed in an SPF animal facility. To establish xenografts, 2×10^6 MDA-MB-231 cells with altered expressions of circUBR5 and/or miR-1179, or corresponding controls were subcutaneously injected into the left flanks of nude mice (N=5/group). Starting from day 6, the length and width of xenografts was measured every four days, with volume calculated as $1/2 \times \text{length} \times \text{width}^2$. On day 30, mice were euthanized with carbon dioxide, and xenografts were isolated, imaged and weighed. The experimental metastasis model was established as described previously [16]. In short, 2×10^5 target MDA-MB-231 cells was injected into the tail vein (N=5/group). After 30 days, all mice were sacrificed by CO₂ exposure and lungs were dissected, photographed, and processed into formalin-fixed paraffin-embedded sections. Hematoxylin and eosin (HE) staining was performed using the H&E Staining Kit (Abcam, Cambridge, MA, USA) according to the instructions from the manufacturer. The quantification of metastatic area was performed using Image J software.

Luciferase reporter assay

Dual-luciferase reporter assay was performed as described earlier [17]. Briefly, wild-type (WT) or mutated (MUT) miR-1179-binding sequence from circUBR5 or UBR5 was cloned into pmir-GLO vector (Promega, Madison, WI, USA), downstream of the firefly luciferase reporter gene. Then the luciferase reporter construct was co-transfected into MDA-MB-231 or BT549 cells together with miR-NC, miR-1179, LNA-NC, or LNA-miR-1179, as well as the control Renilla luciferase vector (Promega) using Lipofectamine 3000 (Invitrogen). After 48 h, firefly and Renilla luciferase activities were measured using Dual-Lumi Luciferase Assay Kit (Beyotime).

RNA immunoprecipitation (RIP)

The interaction between circUBR5 and miR-1179 was examined by Flag-MS2bp-MS2bs-

based RIP assay as described previously [18]. In brief, WT or MUT miR-1179-binding sequence from circUBR5 was cloned into MS2bs vector, and co-transfected into BT549 and MDA-MB-231 cells with Flag-MS2bp vector using Lipofectamine 3000. MS2bs-Renilla was used as the negative control. After 48 h, cell lysate was prepared and IP was performed using anti-Flag M2 magnetic beads (Sigma, St. Louis, MO, USA). The co-precipitated RNA was detected by RT-PCR.

To examine the association of Argonaute 2 (Ago2) with circUBR5, miR-1179, or UBR5 mRNA, cell lysates were prepared from target BT549 and MDA-MB-231 cells and incubated with either anti-Ago2 antibody (ab186733, Abcam) or control IgG (ab109489; negative control) followed by protein A magnetic beads. Both input and precipitated samples were then treated with proteinase K and examined by RT-PCR.

Western blot

Cell lysates were prepared from xenograft tissue or cell lines using RIPA buffer (Beyotime) supplemented with protease and phosphatase inhibitors. Equal amounts of total proteins were separated on SDS-PAGE gel and transferred onto polyvinylidene fluoride membranes. After blocking in TBST buffer containing 5% non-fat milk for 1 h, the membrane was incubated at 4°C overnight with anti-UBR5 (1:1000; ab134089) and anti-GAPDH (1:3000; ab-9485; Abcam). After the incubation with HRP-conjugated secondary antibodies, signals were developed with enhanced chemiluminescence substrate and imaged using LAS400 imaging system (Fujifilm, Tokyo, Japan).

Statistical analysis

Data analysis was performed using SPSS software (version 22.0; IBM, Armonk, NY, USA). *In vitro* experiments were performed in triplicate and repeated three independent times. Data were presented as mean \pm standard deviation ($\bar{x} \pm \text{sd}$) and compared using Student's *t* test between two groups and ANOVA followed by Tukey's post hoc test among multiple groups. Linear association analysis between different target genes was performed using Pearson correlation test. Statistical significance was defined as $P < 0.05$.

Results

Characterization of circUBR5

By far, little is known on circUBR5 (hsa_circ_0001819). Analysis on its genetic information showed that it is derived from human UBR5 gene located in the long arm of chromosome 8 (chr8: 103,372,298-103,373,854; **Figure 1A**). Specifically, circUBR5 is an exonic circRNA generated by the back splicing of exons 2, 3, 4, and 5 from human UBR5 pre-mRNA (**Figure 1B**). Conforming to its circular nature, circUBR5 was more stable than the linear UBR5 mRNA, as evidenced by the significant reduction of UBR5 mRNA, but not circUBR5 upon treating total RNA from MDA-MB-231 cells with RNase R (**Figure 1C**). In addition, the degradation of circUBR5 was drastically slower than that of UBR5 mRNA when the *de novo* gene transcription in MDA-MB-231 cells was blocked by actinomycin D (**Figure 1D**).

Higher expression of circUBR5 is detected in TNBC tumors and correlates with shorter patient survival

To understand the clinical importance of circUBR5 in TNBC, we first compared its expression in 50 pairs of TNBC tissues and ANT breast tissues. As shown in **Figure 2A** circUBR5 level was significantly up-regulated in TNBC tissues, when compared to the matched ANT tissues. Survival analysis showed that a higher expression of circUBR5 in TNBC tissues was associated with shorter overall survival of patients (**Figure 2B**). When comparing its expression among the normal breast epithelial cells (MCF10A) and a panel of BC cell lines, including two non-TNBC (MCF7 and SK-BR-3) and three TNBC cell lines (BT549, MDA-MB-231, and MDA-MB-468), we detected the significant up-regulation of circUBR5 in all BC cell lines than in MCF10A cells. In particular, circUBR5 expression was robustly higher in TNBC than that in non-TNBC lines (**Figure 2C**). Therefore, we focused on BT549 and MDA-MB-231 cells in this study. Fractionation analysis showed that in both cells, the majority of circUBR5 was localized in the cytoplasm (**Figure 2D**), which was corroborated by RNA FISH assay (**Figure 2E**), suggesting that sponging miRNAs could be a potential mechanism mediating its functions. To assess its functional significance, we

generated two siRNAs targeting circUBR5 (si-circUBR5 #1 and #2). Compared to siNC, single si-circUBR5 sequence (100 nM) achieved an approximately 50%-55% knockdown efficiency in both MDA-MD-231 cells and BT549 cells. However, the co-transfection of si-circUBR5 #1 and si-circUBR5 #2 (50 nM for each) reduced circUBR5 expression by nearly 85% (**Figure 2F**). Due to this obvious synergistic effect, a mixture of si-circUBR5 #1 and #2 (50 nM for each) was used for silencing circUBR5 in the following experiments.

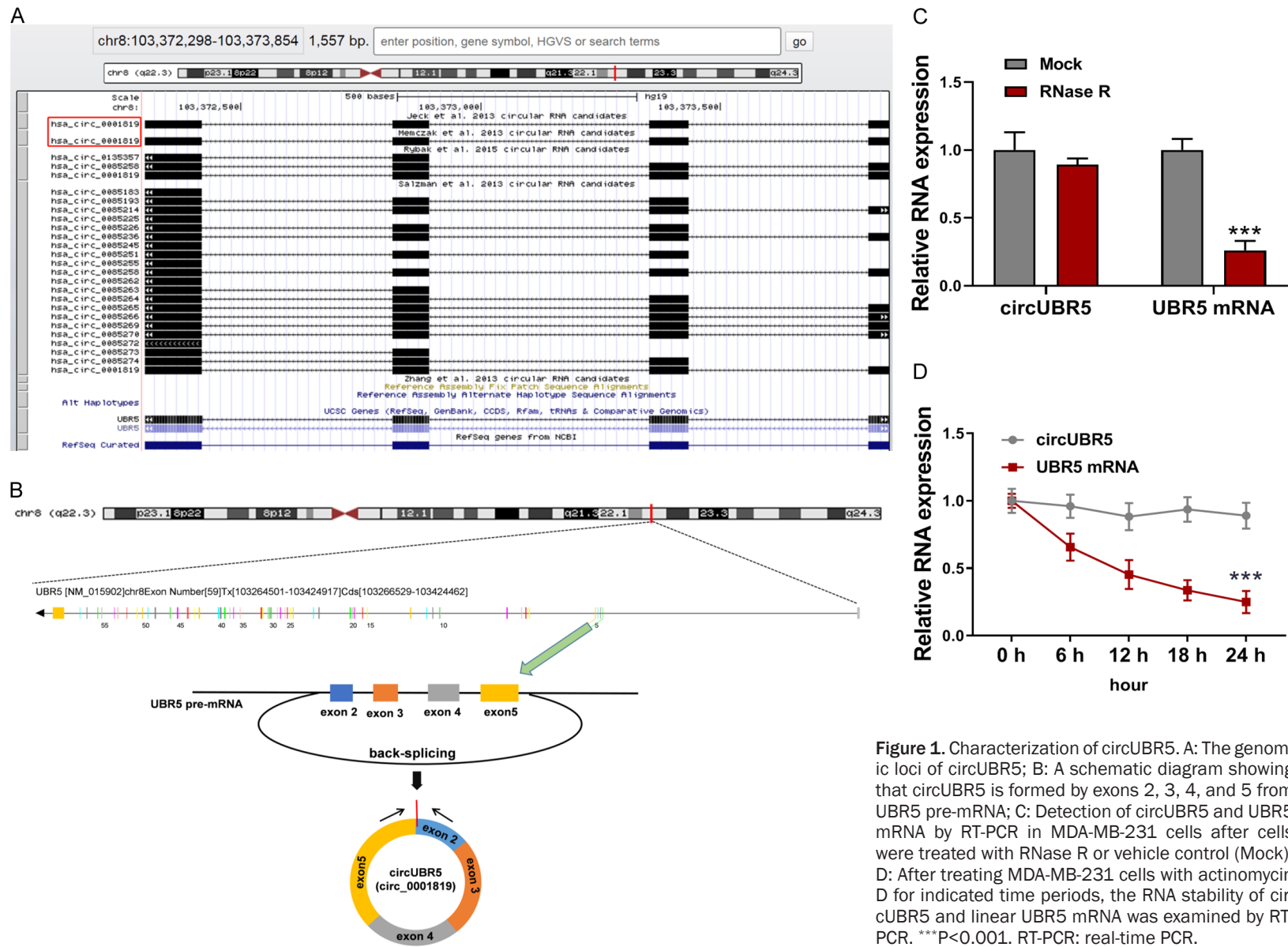
Knocking down circUBR5 inhibits in vitro as well as in vivo malignancy of TNBC cells

To assess the effects of circUBR5 in regulating the malignant phenotypes of TNBC cells, we performed analyses on *in vitro* cell viability (by CCK-8 assay), proliferation (by both colony formation and EdU proliferation assays), motility (by Transwell invasion and wound healing assays), as well as on *in vivo* tumor growth (by xenograft growth) and metastasis (by experimental metastasis assay). When compared to si-NC TNBC cells, si-circUBR5 cells showed significantly reduced *in vitro* viability (**Figure 3A**), long-term proliferation (**Figure 3B**), short-term proliferation (**Figure 3C** and **3D**), invasion (**Figure 3E**), and migration (**Figure 3F**; all $P < 0.01$). In addition, we generated MDA-MB-231 cells stably expressing sh-NC or sh-circUBR5. When injected subcutaneously into nude mice, sh-circUBR5 MDA-MB-231 cells grew much slower *in vivo* (**Figure 3G**), forming significantly smaller and lighter xenografts than the corresponding sh-NC cells (**Figure 3H** and **3I**). Similarly, when injected intravenously, sh-circUBR5 cells generated significantly fewer metastatic foci in lungs than sh-NC cells ($P < 0.01$; **Figure 3J**). HE staining showed that the area of metastatic foci in lung tissue from sh-circUBR5 group was much smaller than that in the sh-NC group (**Figure 3K**). Collectively, these data suggest that circUBR5 essentially maintains multiple malignant phenotypes of TNBCs both *in vitro* and *in vivo*.

CircUBR5 serves as a miRNA sponge for miR-1179

Since a key mechanism by which cytoplasmic circRNAs function is through the circRNA/miRNA/mRNA network, and the majority of circUBR5 is localized in the cytoplasm rather than

The circUBR5/miR-1179/UBR5 axis in TNBC



The circUBR5/miR-1179/UBR5 axis in TNBC

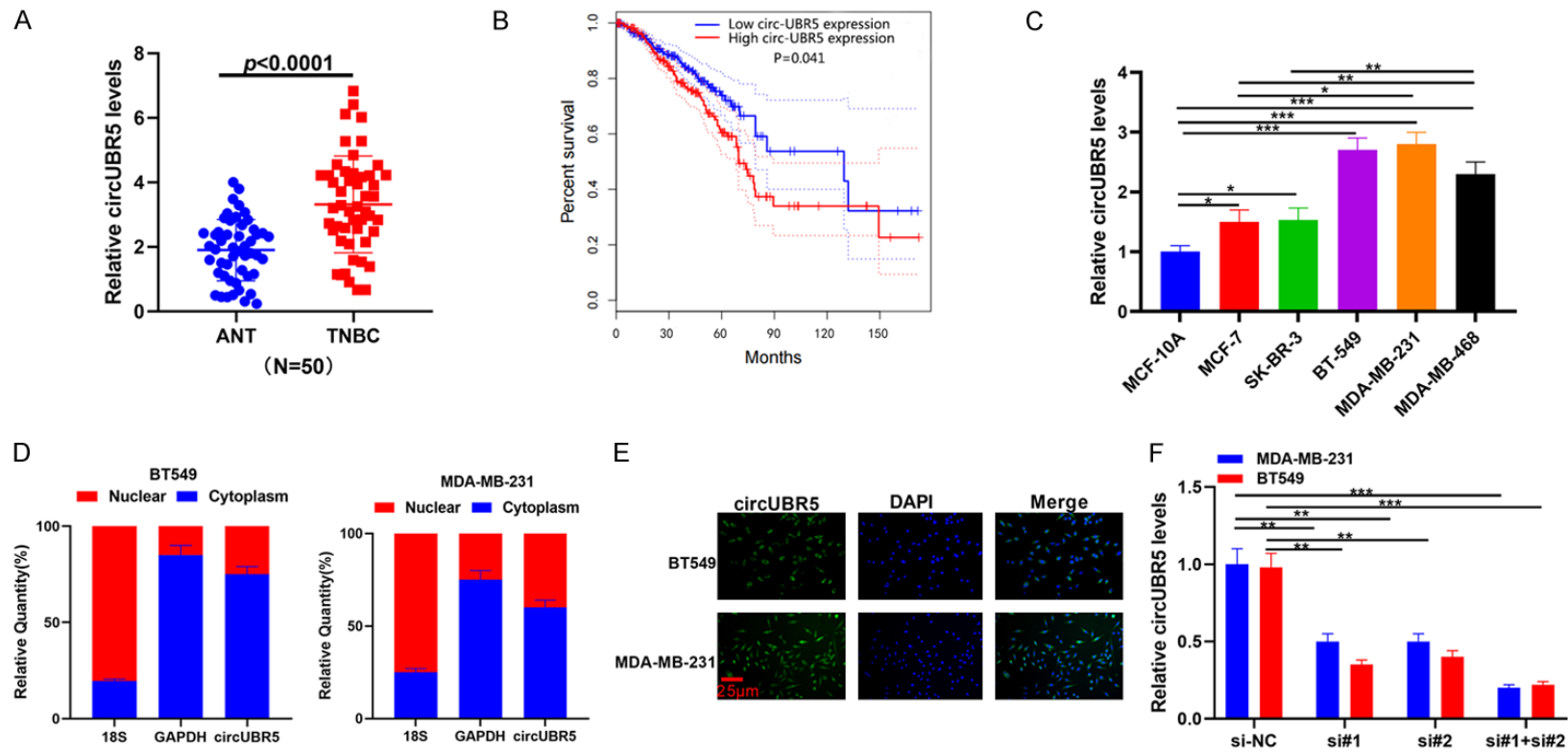
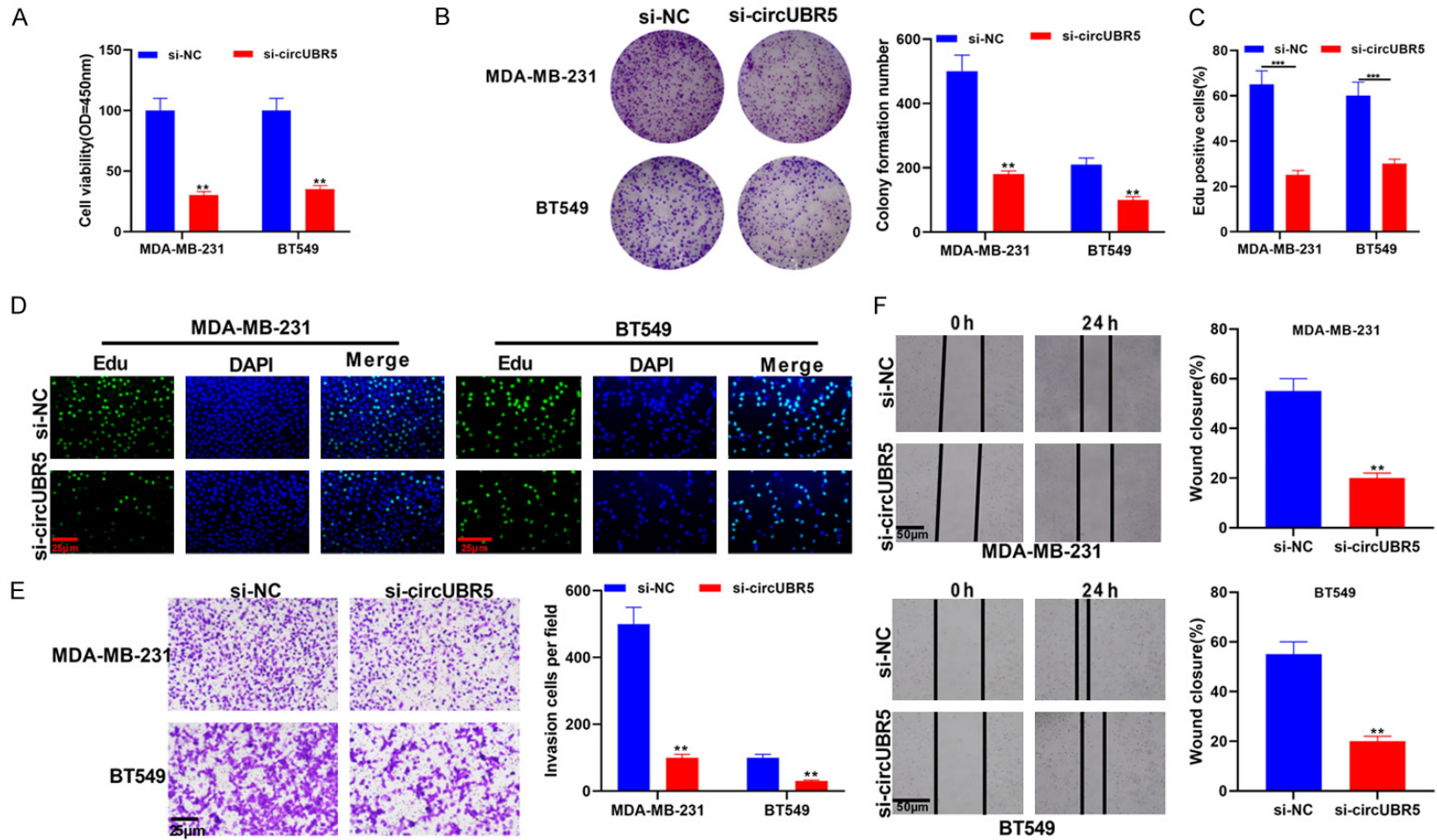


Figure 2. CircUBR5 is up-regulated in TNBC tissues or cells and associated with worse patient prognosis. A: CircUBR5 expression was examined by RT-PCR in 50 matching pairs of TNBC tissues and ANT breast tissues; B: Survival analysis using Kaplan-Meier method examined the association between circUBR5 level and the overall survival of TNBC patients (N=50); C: CircUBR5 expression was examined by RT-PCR in non-tumorigenic breast epithelial cells MCF10A and indicated breast cancer cells; D: Nuclear and cytoplasmic fractions were prepared from BT549 and MDA-MB-231 cells. Expressions of circUBR5, 18S (a marker for the nuclear fraction), and GAPDH (a marker for the cytoplasmic fraction) were examined by RT-PCR and presented as % of relative quantity in indicated fractions; E: RNA FISH assay revealed the cytoplasmic localization of circUBR5 (green signal). Cell nuclei were stained with DAPI (blue signal). Scale bar =25 μ m, magnification =200 \times ; F: BT549 and MDA-MB-231 cells were transfected with si-NC or two different si-circUBR5 (#1 and #2), or #1 plus #2. CircUBR5 expression was examined by RT-PCR. *P<0.05, **P<0.01, ***P<0.001. RT-PCR: real-time PCR; ANT: adjacent non-tumor.

The circUBR5/miR-1179/UBR5 axis in TNBC



The circUBR5/miR-1179/UBR5 axis in TNBC

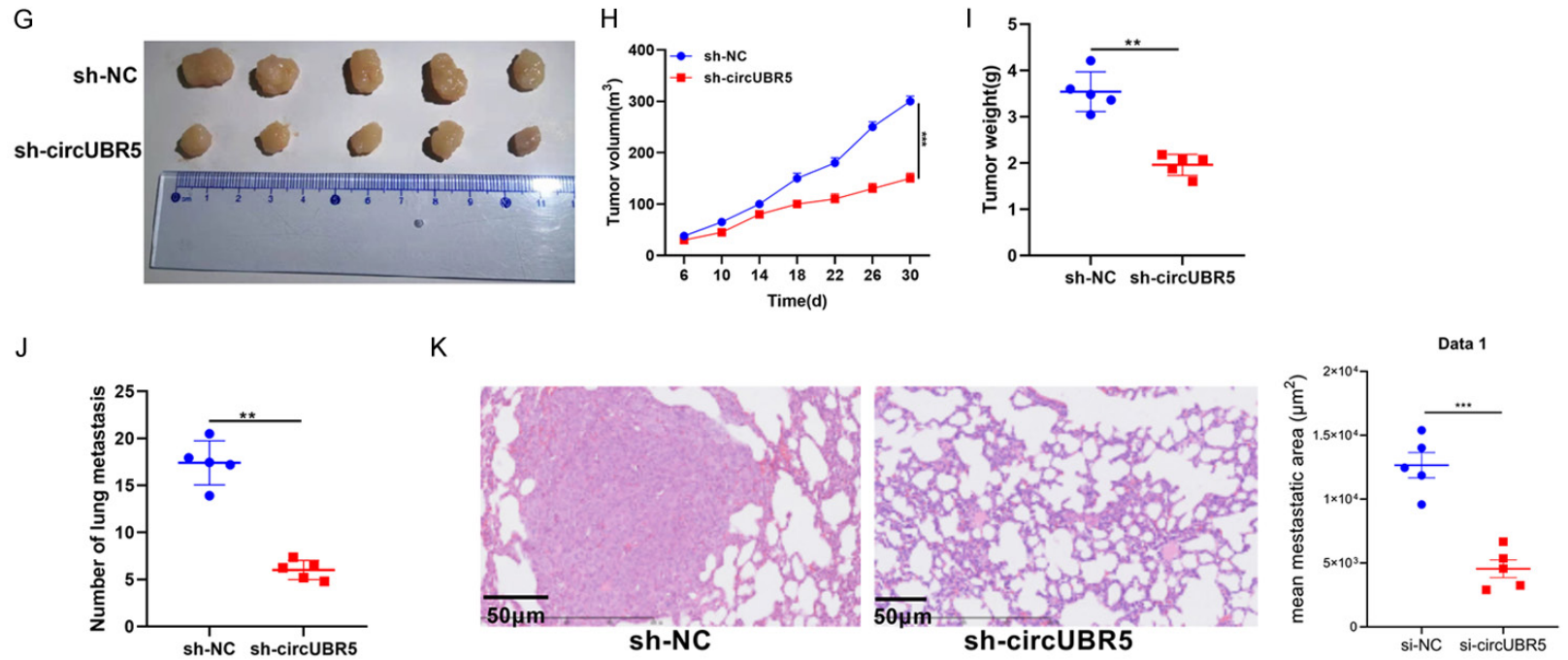


Figure 3. CircUBR5 critically controls the malignancy of TNBC *in vitro* and *in vivo*. BT549 and MDA-MB-231 cells were transfected with si-NC or si-circUBR5. A: Cell viability was examined by CCK-8 assay; B: Long-term proliferation was examined by colony formation assay (left panels) and the colony number was compared between indicated cells (right bar graph); C and D: Short-term proliferation was examined by EdU proliferation assays. EdU⁺ cells were labeled as green and cell nuclei stained with DAPI as blue. Scale bar = 25 μm, magnification = 200×; E: Cell invasion was examined by transwell assay (left), with the average number of invasive cells per field compared between indicated cells. Scale bar = 25 μm, magnification = 200×; F: Cell migration was examined using wound healing assay (left) and the % wound closure was compared between indicated cells (right). Scale bar = 50 μm, magnification = 100×; G, H: Pictures of xenografts derived from sh-NC and sh-circUBR5 MDA-MB-231 cells (N=5/group, left panel), and the growth curve of xenografts *in vivo* (right panel); I: Weight of xenografts derived from indicated MDA-MB-231 cells; J: After intravenous injection of sh-NC and sh-circUBR5 MDA-MB-231 cells (N=5/group), lung tissues were isolated and the number of lung metastasis was compared between indicated groups; K: HE staining was applied to assess the area of metastatic foci in lung tissue. Scale bar = 50 μm, magnification = 200×. **P<0.01. ***P<0.001.

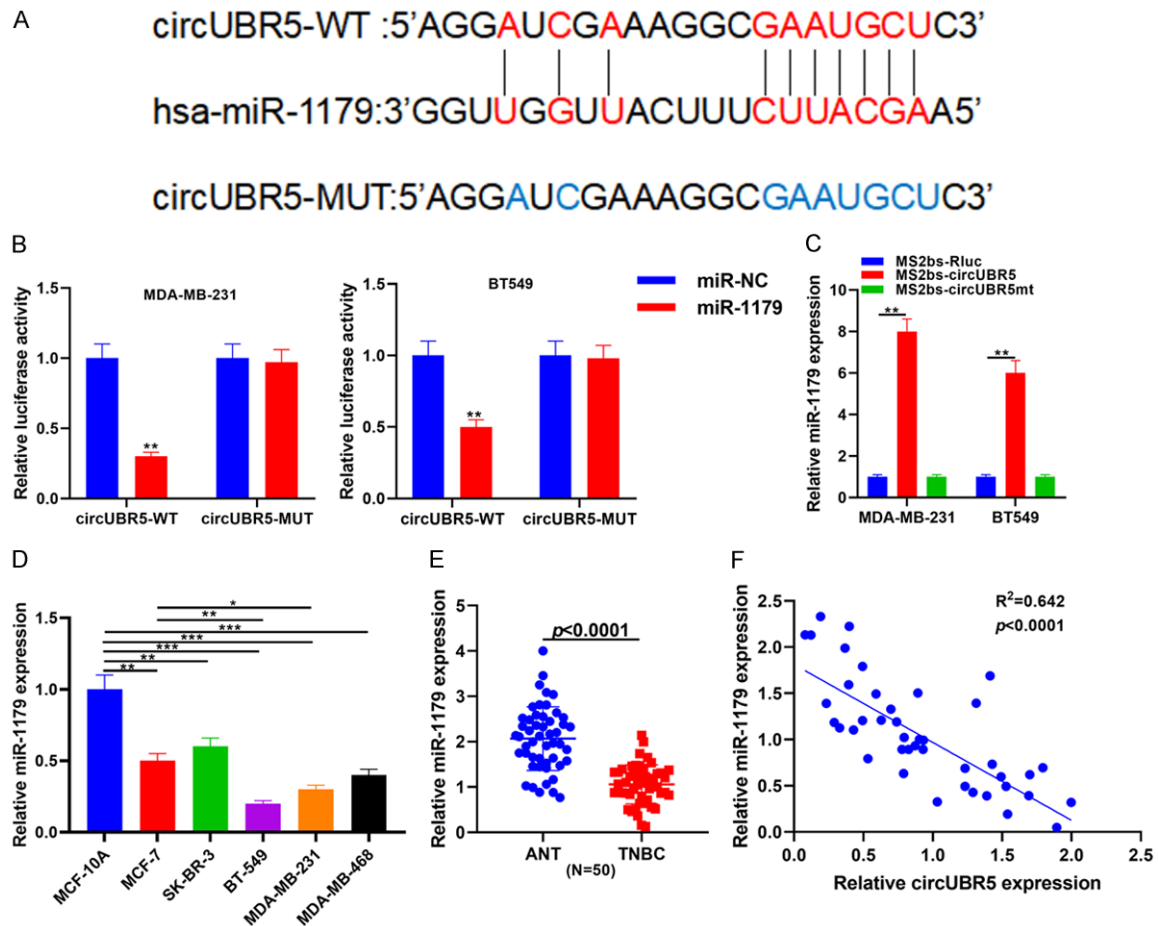


Figure 4. CircUBR5 interacts and down-regulates miR-1179. A: StarBase analysis predicted a potential binding site between circUBR5 and miR-1179; B: BT549 and MDA-MB-231 cells were transfected with reporter construct containing wild-type (WT) or mutated (MUT) miR-1179-binding sequence in circUBR5, together with miR-NC or miR-1179 mimics. Luciferase activity was examined and compared; C: Wild-type (WT) and mutated (MUT) circUBR5 sequence was cloned into MS2bs vector and examined for its interaction with miR-1179 using MS2-based RIP assay. MS2bs-Rluc was used as a negative control; D: Expression of miR-1179 from indicated breast epithelial cells was examined by RT-PCR; E: Expression of miR-1179 was examined by RT-PCR and compared between 50 matching pairs of ANT and TNBC tissues; F: The correlation between circUBR5 and miR-1179 levels in TNBC tissues was analyzed using Pearson correlation test. * $P < 0.05$, ** $P < 0.01$, *** $P < 0.001$. RT-PCR: real-time PCR; ANT: adjacent non-tumor.

the nucleus (**Figure 2D**), we explored the miRNAs that may interact with circUBR5 using StarBase (<http://starbase.sysu.edu.cn/>) and identified miR-1179 as a candidate (**Figure 4A**). By a luciferase reporter assay, we found that miR-1179 mimics specifically inhibited the reporter activity regulated by WT-, but not in MUT-circUBR5 (in which miR-1179-binding sequence was mutated; **Figure 4B**), suggesting this site is critical for the interaction between circUBR5 and miR-1179. Consistently, MS2-based RIP assay showed that the WT sequence specifically interacted with endogenous miR-1179 in both BT549 and MDA-MB-231 cells. In contrast, MUT sequence or negative control sequence (MS2bs-Rluc) failed to do so (**Figure 4C**). Expressional analysis showed that miR-

1179 was significantly down-regulated in all BC cells examined when compared to MCF10A cells, and the most robust reduction was observed in TNBC cell lines (**Figure 4D**). In addition, miR-1179 expression was significantly lower in TNBC than in ANT tissues (**Figure 4E**). Further analysis revealed a negative correlation between circUBR5 and miR-1179 levels in TNBC tissues ($P < 0.001$, $R^2 = 0.719$; **Figure 4F**), supporting that circUBR5 acts as a sponge for miR-1179.

Targeting miR-1179 mediates the oncogenic activities of circUBR5 in TNBC

To evaluate the significance of miR-1179 in circUBR5-induced malignancy of TNBC cells, we

concomitantly silenced both circUBR5 and miR-1179 (si-circUBR5+LNA-miR-1179) in TNBC cells. As shown earlier, si-circUBR5 alone significantly reduced the viability (**Figure 5A**), long-term proliferation (**Figure 5B**), invasion (**Figure 5C**), and migration (**Figure 5D**) of both BT549 and MDA-MB-231 cells. However, all these phenotypes were completely reversed (i.e., to the level comparable to that observed in si-NC cells) in si-circUBR5+LNA-miR-1179 cells, suggesting that sponging miR-1179 mediates the oncogenic activities of circUBR5 in TNBC cells. As expected, miR-1179 expression was significantly up-regulated in si-circUBR5 cells ($P < 0.05$, when compared to si-NC cells), but not in si-circUBR5+LNA-miR-1179 cells ($P > 0.05$, when compared to si-NC cells; **Figure 5E**).

MiR-1179 directly targets UBR5

In addition to predicting the potential binding between circUBR5 and miR-1179, StarBase analysis also revealed that the same sequence in miR-1179 may interact with the 3' untranslated region (3'UTR) of UBR5 mRNA (**Figure 6A**), suggesting UBR5 could be a direct target for miR-1179. Luciferase reporter assay using the UBR5 3'UTR-WT and -MUT sequence showed that miR-1179 mimics specifically inhibited, while LNA-miR-1179 activated the luciferase activity controlled by UBR5 3'UTR-WT, but not UBR5 3'UTR-MUT sequence (**Figure 6B**). Similarly, miR-1179 mimics reduced, while LNA-miR-1179 boosted the expression of endogenous UBR5 at both mRNA (**Figure 6C**) and protein (**Figure 6D**) levels in BT549 and MDA-MB-231 cells. RIP assay using anti-Ago2 antibody, the central component in RNA-induced silencing complex (RISC) showed that when compared to anti-IgG, circUBR5, miR-1179, and UBR5 mRNA were all associated with RISC in both BT549 and MDA-MB-231 cells (**Figure 6E** and **6F**). However, when endogenous circUBR5 was knocked down in both cells by si-circUBR5, the association of RISC with UBR5 mRNA was potently boosted (**Figure 6G**). Consistently, si-circUBR5 effectively reduced UBR5 level in both BT549 and MDA-MB-231 cells, while the concomitant silence of circUBR5 and miR-1179 recovered UBR5 expression (both mRNA in **Figure 6H** and protein in **Figure 6I**) to the level comparable to that in si-NC-transfected cells. When profiling UBR5 expres-

sion in different BC cells, we found that similar to circUBR5, UBR5 expression was significantly up-regulated in all BC cells when compared to that in the normal MCF10A cells, and the highest expression was observed in all three TNBC cells (**Figure 6J**). The expressional difference was also noted between TNBC tissues and ANT tissues (**Figure 6K**). Collectively, these findings suggest that miR-1179 directly targets UBR5 mRNA to RISC-induced degradation. By sponging miR-1179, circUBR5 up-regulates UBR5 expression.

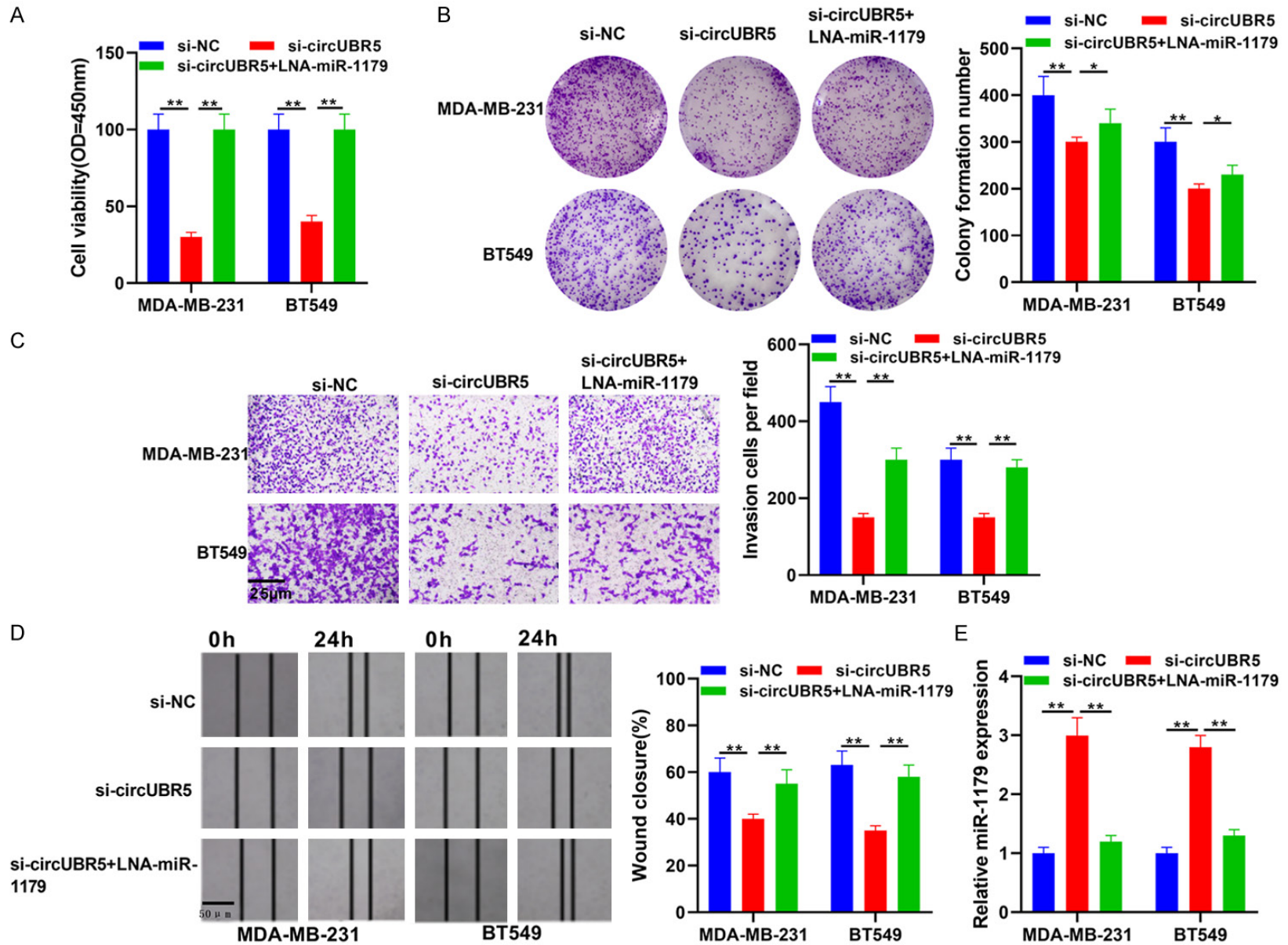
UBR5 critically mediates the tumor-regulating activities of circUBR5 and miR-1179

To assess the importance of UBR5 in circUBR5- and miR-1179-regulated malignancy of TNBC cells, we either overexpressed UBR5 in si-circUBR5-transfected TNBC cells (si-circUBR5+UBR5) or simultaneously silenced miR-1179 and UBR5 in TNBC cells (LNA-miR-1179+si-UBR5). Expressional analysis showed that si-circUBR5 significantly reduced endogenous UBR5 level, which was recovered in si-circUBR5+UBR5 cells (**Figure 7A**). Functionally, knocking down circUBR5 alone inhibited malignant behaviors, including viability (**Figure 7B**), long-term proliferation (**Figure 7C**), invasion (**Figure 7D**), and migration (**Figure 7E**) in both BT549 and MDA-MB-231 cells. Overexpressing UBR5 in these cells, however, negated all anti-cancer benefits of si-circUBR5. On the other hand, the expression of endogenous UBR5 was markedly increased in LNA-miR-1179 cells but returned to the basal level in LNA-miR-1179+si-UBR5 cells (**Figure 7F**). Correspondingly, LNA-miR-1179-transfected TNBC cells demonstrated enhanced malignancy, as represented by increased viability (**Figure 7G**), long-term proliferation (**Figure 7H**), invasion (**Figure 7I**), and migration (**Figure 7J**), when compared to LNA-NC cells, which were all rescued by knocking down UBR5 in these LNA-miR-1179-transfected TNBC cells. Together, these data suggest the essential role of UBR5 in circUBR5- and miR-1179-regulated malignant phenotypes of TNBC.

CircUBR5/miR-1179 axis regulates the in vivo growth and metastasis of TNBC cells

Lastly, to examine whether the *in vitro* effects of circUBR5/miR-1179 can be translated *in vivo*, we measured the xenograft growth and

The circUBR5/miR-1179/UBR5 axis in TNBC



The circUBR5/miR-1179/UBR5 axis in TNBC

Figure 5. Targeting miR-1179 mediates the oncogenic phenotypes of circUBR5. BT549 and MDA-MB-231 cells were transfected with si-NC, si-circUBR5, or si-circUBR5+LNA-miR-1179 inhibitor. A: Cell viability was examined by CCK-8 assay and compared between indicated cells; B: Long-term proliferation was examined by colony formation assay (left panels) and the colony formation number was compared between indicated cells (right bar graph); C: Cell invasion was examined by transwell assay (left), with the average number of invasive cells per field compared between indicated cells. Scale bar =25 μ m, magnification =200 \times ; D: Cell migration was examined using wound healing assay (left) and the % wound closure was compared between indicated cells (right). Scale bar =50 μ m, magnification =100 \times ; E: Expression of miR-1179 was examined by RT-PCR in indicated group of cells. *P<0.05, **P<0.01, ***P<0.001. RT-PCR: real-time PCR.

metastasis of MDA-MB-231 cells stably expressing sh-circUBR5, with or without simultaneous targeting miR-1179. First, levels of circUBR5 and miR-1179 were assessed in xenograft tissues, which showed the efficacy of sh-circUBR5 in down-regulating circUBR5 while up-regulating miR-1179, and that of miR-1179 inhibitor in reducing miR-1179 only (**Figure 8A** and **8B**). As shown earlier, sh-circUBR5 significantly inhibited xenograft tumor growth (**Figure 8C-E**) and lung metastasis (**Figure 8F**) of MDA-MB-231 cells when compared to sh-NC cells. In contrast, miR-1179 inhibitor abolished the *in vivo* tumor suppressive activities of sh-circUBR5, restoring both the xenograft growth and lung metastasis to the levels generated by sh-NC cells, suggesting that sponging miR-1179 mediates the *in vivo* oncogenic phenotypes of circUBR5.

Discussion

In this study, we expand our understanding by showing that circUBR5 (hsa_circ_0001819) presents oncogenic activities in TNBC. CircUBR5 expression was not only up-regulated in TNBC tissues or cells, but also associated with shorter overall survival of TNBC patients. *In vitro*, circUBR5, by sponging miR-1179 and up-regulating UBR5, was essential for sustaining the proliferation and motility of TNBC cells. Similarly, silencing circUBR5 led to the impaired xenograft growth and metastasis *in vivo* (**Figure 8G**). Consequently, this study highlights the potential of targeting circUBR5 in treating TNBC.

CircRNAs act through distinct mechanisms depending on their subcellular localizations. In the nucleus, circRNAs may directly regulate gene transcription or ribosomal RNA maturation [19, 20]. In the cytoplasm, circRNAs could decoy proteins to influence their functions [21-23]. However, the most common mechanism of action for circRNAs is serving as miRNA spong-

es in the cytoplasm and modulating the circRNA/miRNA/mRNA network [24]. This is also the most frequently identified mechanism responsible for the pro- or anti-tumor activities of circRNAs in TNBC. For example, circANKS1B sponged miR-148a-3p and miR-152-3p to up-regulate the expression of transcription factor USF1 and promoted TNBC metastasis; circEPSTI1 acted as a sponge for miR-4753 and miR-6809 to elevate BCL11A expression and stimulated TNBC growth; the circAGFG1/miR-195-5p/CCNE1 axis aggravated tumorigenesis and metastasis in TNBC [25-27]. In contrast, some other circRNAs act as tumor suppressors in TNBC, such as the circTADA2A-E6/miR-203a-3p/SOCS3 axis and the circFBXW7/miR-197-3p/FBXW7 axis [28, 29].

By far, the only study on the biological significance of circUBR5 (hsa_circ_0001819) is reported by Luan et al., who found the up-regulated circUBR5 expression in lupus nephritis [30]. Our present work is therefore the first study demonstrating the oncogenic activities of circUBR5 in human cancer. The up-regulation of circUBR5 in TNBC tissues and its negative association with patient survival suggest its potential as a prognostic biomarker. In addition, we detected an elevated expression of circUBR5 in non-TNBC breast cancer cells (MCF-7 and SK-BR3) than in normal breast epithelial MCF10A cells, despite a more robust increase in TNBC cell lines. Therefore, further studies should be performed to examine whether circUBR5 serves as a unique prognostic biomarker for TNBC or for breast cancer in general. The predominant distribution of circUBR5 in the cytoplasm is consistent with its miRNA-sponging function. Interestingly, another circUBR5 derived from exon 35-36 of UBR5 gene was mostly found in the nucleus, down-regulated in non-small cell lung cancer, and not associated with the expression of parent gene UBR5, suggesting that the same parent gene may generate structurally and functionally distinct cir-

The circUBR5/miR-1179/UBR5 axis in TNBC

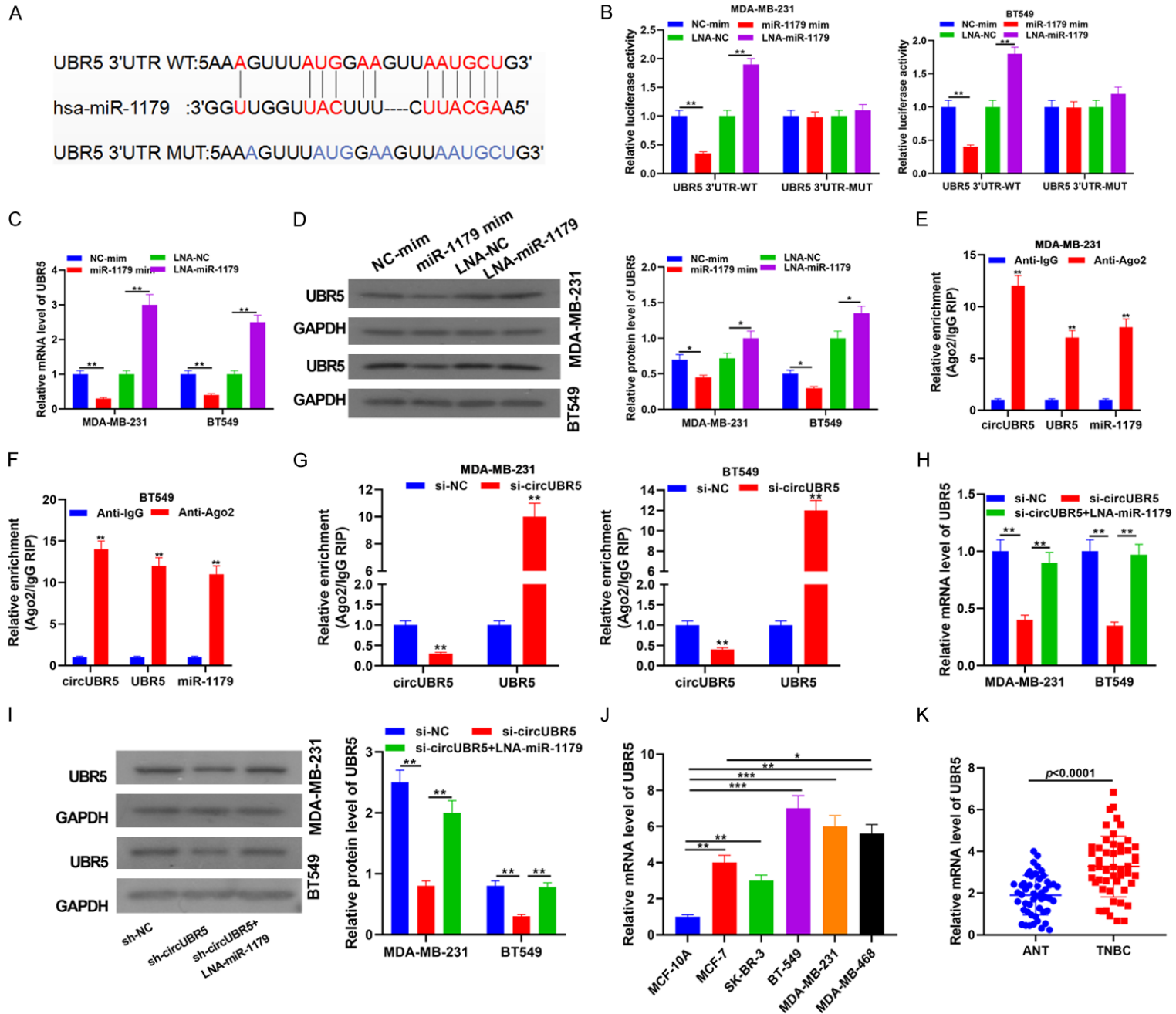


Figure 6. UBR5 is a direct target of miR-1179; circUBR5, by sponging miR-1179, up-regulates UBR5 in TNBC cells. A: StarBase analysis revealed a potential binding site between miR-1179 and UBR5; B: WT or MUT miR-1179-binding sequence in UBR5 3'UTR was cloned into luciferase construct, co-transfected into BT549 and MDA-MB-231 cells with miR-1179 vs. miR-NC or LNA-miR-1179 vs. LNA-NC, and examined for luciferase activity; C and D: Expression of UBR5 on mRNA and protein levels were examined by RT-PCR and Western blot, respectively; E and F: RIP assay examined the association of Ago2 with endogenous circUBR5, miR-1179, and UBR5 mRNA, respectively; G: Upon transfecting BT549 and MDA-MB-231 cells with si-NC or si-circUBR5, the association of Ago2 with circUBR5 and UBR5 mRNA was examined by RIP assay; H: BT549 and MDA-MB-231 cells were transfected with si-NC, si-circUBR5, or si-circUBR5+LNA-miR-1179 inhibitor; I: Relative expression of UBR mRNA and protein was examined by RT-PCR and Western blot, respectively; J: Expression of UBR5 from indicated breast epithelial cells was examined by RT-PCR; K: Expression of UBR5 was examined by RT-PCR and compared between 50 matching pairs of normal and TNBC tissues. *P<0.05, **P<0.01, ***P<0.001. RT-PCR: RNA stability and real-time PCR; WT: wild-type; MUT: mutated.

crNAs [31]. Considering the limited information available for these two circUBR5, further studies should be performed to examine regulations on their expressions, intracellular localizations, and potential crosstalk with each other.

In contrast to the limited information available for circUBR5, miR-1179 has been extensively studied and characterized as a tumor suppressor in various human cancers. The downstream mechanisms mediating the anti-cancer activities of miR-1179, however, seem to vary greatly. For example, miR-1179 was reported to target HMGB1 in gastric cancer and thyroid cancer, suppress E2F5 in pancreatic cancer, inhibit PI3K/Akt signaling in ovarian cancer and oral cancer, and CDK2 in cervical cancer [32-37]. The upstream regulators of miR-1179 are equally diversified. Therefore, miR-1179 may serve as a signaling hub connecting various upstream stimuli with a repertoire of downstream effectors. MiR-1179 has been reported to target Notch signaling and inhibit breast cancer metastasis [38]. In this study, we revealed that sponging miR-1179 mediated the positive regulation of circUBR5 on its parent gene UBR5. This mechanism was further supported by the negative correlation between circUBR5 and miR-1179 expression in TNBC tissues. Functionally, this signaling mediated the oncogenic activities of circUBR5 since the concomitant silencing of miR-1179 abolished the *in vitro* and *in vivo* phenotypes of si-circUBR5. The parent gene for circUBR5 also encodes a protein product UBR5, a E3 ubiquitin ligase that is highly conserved across metazoan species. UBR5 regulates multiple biological processes, and is frequently overexpressed in cancer [39]. Functionally, UBR5 promotes a variety of malignancy-related phenotypes, including growth, metastasis, angiogenesis, immune escape, and drug resistance [10-13]. In breast cancer,

gene amplification has been identified as a mechanism responsible for the up-regulation of UBR5 [14, 40, 41]. Here we revealed a novel mechanism that circUBR5-induced sponging of miR-1179 up-regulated UBR5. Consequently, the circUBR5/miR-1179/UBR5 axis provides a positive feedback loop to further boost UBR5 expression in TNBC cells. Employing dual and positive feedback mechanisms to ensure the overexpression of UBR5 is a strong indicator for its biological significance in TNBC, which justifies the strategies to target this signaling in suppressing TNBC progression, as corroborated by our *in vitro* and *in vivo* findings. In addition, given the variety of cancer-related phenotypes regulated by UBR5, it is interesting for future studies to explore the biological processes critical for TNBC malignancy and regulated by circUBR5, other than those examined here.

In this study, we mainly focused on the growth and motility of TNBC cells. However, considering that many other biological processes such as angiogenesis, immune responses, cancer stemness, and drug resistance all contribute to the malignancy of TNBC, it would be critical to examine whether circUBR5 may also impact these phenotypes and if so, whether the miR-1179/UBR5 axis is involved [42-45]. Furthermore, we focused on miR-1179 and UBR5 in this study. It would be interesting to explore other miRNAs that might be regulated by circUBR5, which will help to determine if circUBR5 is a regulatory hub driving the malignancy of TNBC.

In summary, we reveal the elevated expression of circUBR5 in TNBC and its association with poor prognosis. By acting as a ceRNA for miR-1179, circUBR5 up-regulates its parent gene, UBR5, an oncogene in TNBC as well as other cancers. This study provides the first evidence that circUBR5 serves as a prognostic biomark-

The circUBR5/miR-1179/UBR5 axis in TNBC

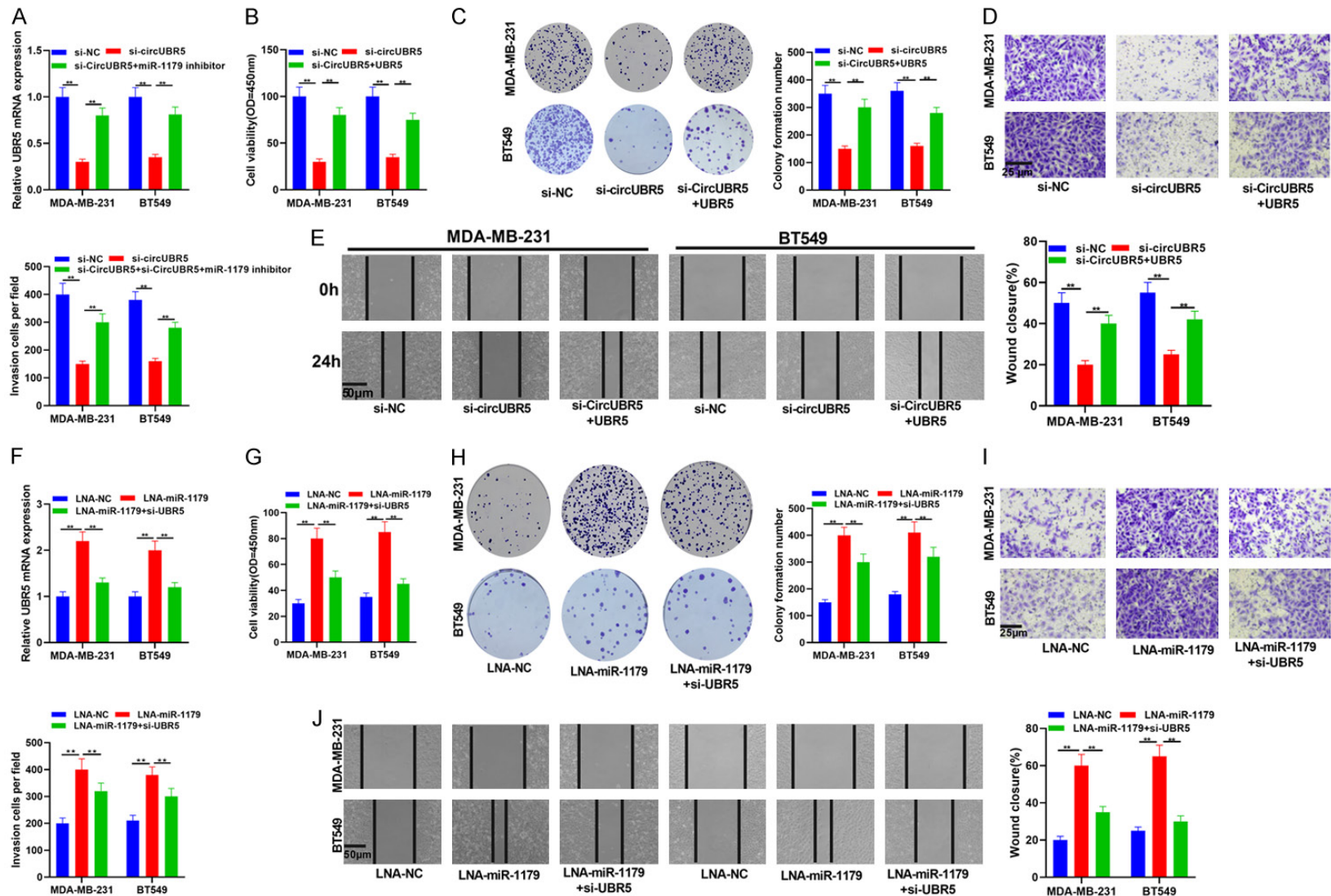


Figure 7. UBR5 critically mediates circUBR5- and miR-1179-regulated oncogenic phenotypes of TNBC cells. BT549 and MDA-MB-231 cells were transfected with si-NC, si-circUBR5, or si-circUBR5+UBR5 (A through E), or with LNA-NC, LNA-miR-1179, or LNA-miR-1179+si-UBR5 (F through J). A and F: Expression of UBR5 was examined by RT-PCR; B and G: Cell viability was examined by CCK-8 assay; C and H: Long-term proliferation was examined and the number of colonies was compared between indicated cells; D and I: Cell invasion was examined by transwell assay, with the average number of invasive cells per field compared between indicated cells. Scale bar =25 μ m, magnification =200 \times ; E and J: Cell migration was examined using wound healing assay and the % wound closure was compared between indicated cells. Scale bar =50 μ m, magnification =100 \times ; **P<0.01. RT-PCR: real-time PCR.

The circUBR5/miR-1179/UBR5 axis in TNBC

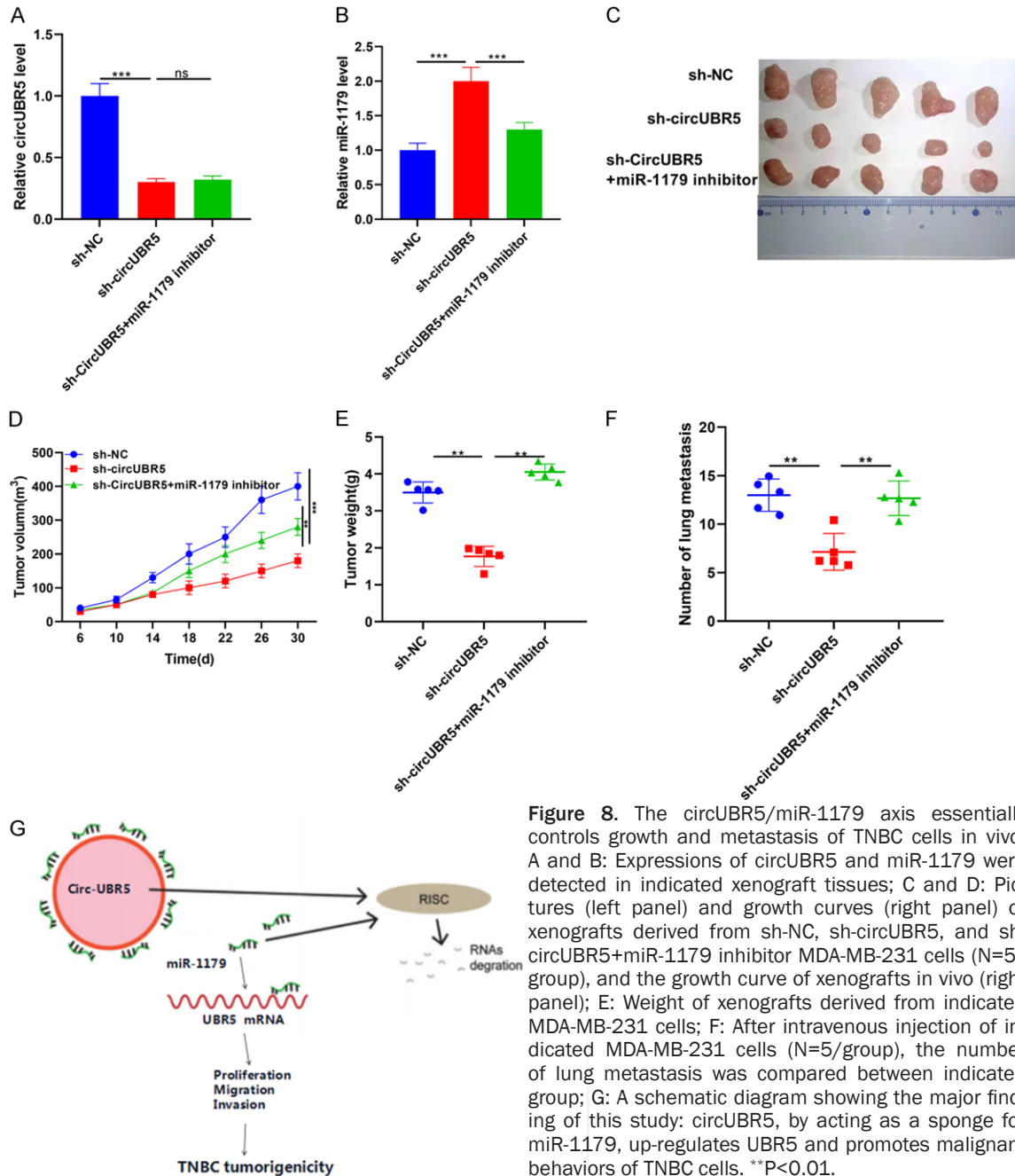


Figure 8. The circUBR5/miR-1179 axis essentially controls growth and metastasis of TNBC cells in vivo. A and B: Expressions of circUBR5 and miR-1179 were detected in indicated xenograft tissues; C and D: Pictures (left panel) and growth curves (right panel) of xenografts derived from sh-NC, sh-circUBR5, and sh-circUBR5+miR-1179 inhibitor MDA-MB-231 cells (N=5/group), and the growth curve of xenografts in vivo (right panel); E: Weight of xenografts derived from indicated MDA-MB-231 cells; F: After intravenous injection of indicated MDA-MB-231 cells (N=5/group), the number of lung metastasis was compared between indicated group; G: A schematic diagram showing the major finding of this study: circUBR5, by acting as a sponge for miR-1179, up-regulates UBR5 and promotes malignant behaviors of TNBC cells. **P<0.01.

er as well as a candidate therapeutical target for TNBC. Considering that UBR5 is an oncogene for a panel of human cancers, future studies may also assess the significance and the therapeutic potential of circUBR5/miR-1179/UBR5 in other cancers.

Acknowledgements

This work was supported by the National Natural Science Foundation of China (818733-73) and Young Innovative and Entrepreneurial

Talents of “Grassland Talents” Project of Inner Mongolia Autonomous Region (Q2017042).

Disclosure of conflict of interest

None.

Address correspondence to: Guohua Gong, Inner Mongolia Key Laboratory of Mongolian Medicine Pharmacology for Cardio-Cerebral Vascular System, First Clinical Medical of Inner Mongolia Minzu University, No. 1742 Holin River Street, Tongliao

028002, Inner Mongolia, P. R. China. Tel: +86-0475-8314245; Fax: +86-0475-8314245; E-mail: Guohuagong16@outlook.com

References

- [1] Mehanna J, Haddad FG, Eid R, Lambertini M and Kourie HR. Triple-negative breast cancer: current perspective on the evolving therapeutic landscape. *Int J Womens Health* 2019; 11: 431-437.
- [2] Bianchini G, Balko JM, Mayer IA, Sanders ME and Gianni L. Triple-negative breast cancer: challenges and opportunities of a heterogeneous disease. *Nat Rev Clin Oncol* 2016; 13: 674-690.
- [3] Su M, Xiao Y, Ma J, Tang Y, Tian B, Zhang Y, Li X, Wu Z, Yang D, Zhou Y, Wang H, Liao Q and Wang W. Circular RNAs in cancer: emerging functions in hallmarks, stemness, resistance and roles as potential biomarkers. *Mol Cancer* 2019; 18: 90.
- [4] Kristensen LS, Andersen MS, Stagsted LVW, Ebbesen KK, Hansen TB and Kjems J. The biogenesis, biology and characterization of circular RNAs. *Nat Rev Genet* 2019; 20: 675-691.
- [5] He D, Yang X, Kuang W, Huang G, Liu X and Zhang Y. The novel circular RNA Circ-PGAP3 promotes the proliferation and invasion of triple negative breast cancer by regulating the miR-330-3p/Myc axis. *Onco Targets Ther* 2020; 13: 10149-10159.
- [6] Li Y, Shi P, Zheng T, Ying Z and Jiang D. Circular RNA hsa_circ_0131242 promotes triple-negative breast cancer progression by sponging hsa-miR-2682. *Onco Targets Ther* 2020; 13: 4791-4798.
- [7] Pei X, Zhang Y, Wang X, Xue B, Sun M and Li H. Circular RNA circ-ZEB1 acts as an oncogene in triple negative breast cancer via sponging miR-448. *Int J Biochem Cell Biol* 2020; 126: 105798.
- [8] Zhou Y, Liu X, Lan J, Wan Y and Zhu X. Circular RNA circRPPH1 promotes triple-negative breast cancer progression via the miR-556-5p/YAP1 axis. *Am J Transl Res* 2020; 12: 6220-6234.
- [9] Shao T, Pan YH and Xiong XD. Circular RNA: an important player with multiple facets to regulate its parental gene expression. *Mol Ther Nucleic Acids* 2021; 23: 369-376.
- [10] Eblen ST and Bradley A. MOAP-1, UBR5 and cisplatin resistance in ovarian cancer. *Transl Cancer Res* 2017; 6: S18-S21.
- [11] Ji SQ, Zhang YX and Yang BH. UBR5 promotes cell proliferation and inhibits apoptosis in colon cancer by destabilizing P21. *Pharmazie* 2017; 72: 408-413.
- [12] Matsuura K, Huang NJ, Cocce K, Zhang L and Kornbluth S. Downregulation of the proapoptotic protein MOAP-1 by the UBR5 ubiquitin ligase and its role in ovarian cancer resistance to cisplatin. *Oncogene* 2017; 36: 1698-1706.
- [13] Song M, Yeku OO, Rafiq S, Purdon T, Dong X, Zhu L, Zhang T, Wang H, Yu Z, Mai J, Shen H, Nixon B, Li M, Brentjens RJ and Ma X. Tumor derived UBR5 promotes ovarian cancer growth and metastasis through inducing immunosuppressive macrophages. *Nat Commun* 2020; 11: 6298.
- [14] Liao L, Song M, Li X, Tang L, Zhang T, Zhang L, Pan Y, Chouchane L and Ma X. E3 Ubiquitin ligase UBR5 drives the growth and metastasis of triple-negative breast cancer. *Cancer Res* 2017; 77: 2090-2101.
- [15] Liang CC, Park AY and Guan JL. In vitro scratch assay: a convenient and inexpensive method for analysis of cell migration in vitro. *Nat Protoc* 2007; 2: 329-333.
- [16] Yang S, Zhang JJ and Huang XY. Mouse models for tumor metastasis. *Methods Mol Biol* 2012; 928: 221-228.
- [17] Ma HY, Li Y, Yin HZ, Yin H, Qu YY and Xu QY. TNFAIP8 promotes cisplatin chemoresistance in triple-negative breast cancer by repressing p53-mediated miR-205-5p expression. *Mol Ther Nucleic Acids* 2020; 22: 640-656.
- [18] Hou P, Zhao Y, Li Z, Yao R, Ma M, Gao Y, Zhao L, Zhang Y, Huang B and Lu J. LincRNA-ROR induces epithelial-to-mesenchymal transition and contributes to breast cancer tumorigenesis and metastasis. *Cell Death Dis* 2014; 5: e1287.
- [19] Holdt LM, Stahring A, Sass K, Pichler G, Kulak NA, Wilfert W, Kohlmaier A, Herbst A, Northoff BH, Nicolaou A, Gabel G, Beutner F, Scholz M, Thiery J, Musunuru K, Krohn K, Mann M and Teupser D. Circular non-coding RNA ANRIL modulates ribosomal RNA maturation and atherosclerosis in humans. *Nat Commun* 2016; 7: 12429.
- [20] Li Z, Huang C, Bao C, Chen L, Lin M, Wang X, Zhong G, Yu B, Hu W, Dai L, Zhu P, Chang Z, Wu Q, Zhao Y, Jia Y, Xu P, Liu H and Shan G. Exon-intron circular rnas regulate transcription in the nucleus. *Nat Struct Mol Biol* 2015; 22: 256-264.
- [21] Du WW, Fang L, Yang W, Wu N, Awan FM, Yang Z and Yang BB. Induction of tumor apoptosis through a circular RNA enhancing Foxo3 activity. *Cell Death Differ* 2017; 24: 357-370.
- [22] Du WW, Yang W, Chen Y, Wu ZK, Foster FS, Yang Z, Li X and Yang BB. Foxo3 circular RNA promotes cardiac senescence by modulating multiple factors associated with stress and senescence responses. *Eur Heart J* 2017; 38: 1402-1412.
- [23] Du WW, Yang W, Liu E, Yang Z, Dhaliwal P and Yang BB. Foxo3 circular RNA retards cell cycle progression via forming ternary complexes

The circUBR5/miR-1179/UBR5 axis in TNBC

- with p21 and CDK2. *Nucleic Acids Res* 2016; 44: 2846-2858.
- [24] Yu CY and Kuo HC. The emerging roles and functions of circular RNAs and their generation. *J Biomed Sci* 2019; 26: 29.
- [25] Chen B, Wei W, Huang X, Xie X, Kong Y, Dai D, Yang L, Wang J, Tang H and Xie X. circEPSTI1 as a prognostic marker and mediator of triple-negative breast cancer progression. *Theranostics* 2018; 8: 4003-4015.
- [26] Yang R, Xing L, Zheng X, Sun Y, Wang X and Chen J. The circRNA circAGFG1 acts as a sponge of miR-195-5p to promote triple-negative breast cancer progression through regulating CCNE1 expression. *Mol Cancer* 2019; 18: 4.
- [27] Zeng K, He B, Yang BB, Xu T, Chen X, Xu M, Liu X, Sun H, Pan Y and Wang S. The pro-metastasis effect of circANKS1B in breast cancer. *Mol Cancer* 2018; 17: 160.
- [28] Xu JZ, Shao CC, Wang XJ, Zhao X, Chen JQ, Ouyang YX, Feng J, Zhang F, Huang WH, Ying Q, Chen CF, Wei XL, Dong HY, Zhang GJ and Chen M. circTADA2As suppress breast cancer progression and metastasis via targeting miR-203a-3p/SOCS3 axis. *Cell Death Dis* 2019; 10: 175.
- [29] Ye F, Gao G, Zou Y, Zheng S, Zhang L, Ou X, Xie X and Tang H. circFBXW7 inhibits malignant progression by sponging miR-197-3p and encoding a 185-aa protein in triple-negative breast cancer. *Mol Ther Nucleic Acids* 2019; 18: 88-98.
- [30] Luan J, Jiao C, Kong W, Fu J, Qu W, Chen Y, Zhu X, Zeng Y, Guo G, Qi H, Yao L, Pi J, Wang L and Zhou H. circHLA-C plays an important role in lupus nephritis by sponging miR-150. *Mol Ther Nucleic Acids* 2018; 10: 245-253.
- [31] Qin M, Wei G and Sun X. Circ-UBR5: An exonic circular RNA and novel small nuclear RNA involved in RNA splicing. *Biochem Biophys Res Commun* 2018; 503: 1027-1034.
- [32] Li Y and Qin C. MiR-1179 Inhibits the proliferation of gastric cancer cells by targeting HMGB1. *Hum Cell* 2019; 32: 352-359.
- [33] Ye M, Hou H, Shen M, Dong S and Zhang T. Circular RNA circFOX1 plays a role in papillary thyroid carcinoma by sponging miR-1179 and regulating HMGB1 expression. *Mol Ther Nucleic Acids* 2020; 19: 741-750.
- [34] Lin C, Hu Z, Yuan G, Su H, Zeng Y, Guo Z, Zhong F, Jiang K and He S. MicroRNA-1179 inhibits the proliferation, migration and invasion of human pancreatic cancer cells by targeting E2F5. *Chem Biol Interact* 2018; 291: 65-71.
- [35] Gao Y, Xu H and Pu T. MicroRNA-1179 suppresses the proliferation and enhances vincristine sensitivity of oral cancer cells via induction of apoptosis and modulation of MEK/ERK and PI3K/AKT signalling pathways. *AMB Express* 2020; 10: 149.
- [36] Zhihong Z, Rubin C, Liping L, Anpeng M, Hui G, Yanting W and Zhenxiu S. MicroRNA-1179 regulates proliferation and chemosensitivity of human ovarian cancer cells by targeting the PTEN-mediated PI3K/AKT signaling pathway. *Arch Med Sci* 2020; 16: 907-914.
- [37] Qu X, Zhu L, Song L and Liu S. circ_0084927 promotes cervical carcinogenesis by sponging miR-1179 that suppresses CDK2, a cell cycle-related gene. *Cancer Cell Int* 2020; 20: 333.
- [38] Li WJ, Xie XX, Bai J, Wang C, Zhao L and Jiang DQ. Increased expression of miR-1179 inhibits breast cancer cell metastasis by modulating notch signaling pathway and correlates with favorable prognosis. *Eur Rev Med Pharmacol Sci* 2018; 22: 8374-8382.
- [39] Shearer RF, Iconomou M, Watts CK and Saunders DN. Functional roles of the E3 ubiquitin ligase UBR5 in cancer. *Mol Cancer Res* 2015; 13: 1523-1532.
- [40] Clancy JL, Henderson MJ, Russell AJ, Anderson DW, Bova RJ, Campbell IG, Choong DY, MacDonald GA, Mann GJ, Nolan T, Brady G, Olopade OI, Woollatt E, Davies MJ, Segara D, Hacker NF, Henshall SM, Sutherland RL and Watts CK. EDD, the human orthologue of the hyperplastic discs tumour suppressor gene, is amplified and overexpressed in cancer. *Oncogene* 2003; 22: 5070-5081.
- [41] Qiao X, Liu Y, Prada ML, Mohan AK, Gupta A, Jaiswal A, Sharma M, Merisaari J, Haikala HM, Talvinen K, Yetukuri L, Pylvanainen JW, Klefstrom J, Kronqvist P, Meinander A, Aittokallio T, Hietakangas V, Eilers M and Westermarck J. UBR5 is coamplified with MYC in breast tumors and encodes an ubiquitin ligase That Limits MYC-dependent apoptosis. *Cancer Res* 2020; 80: 1414-1427.
- [42] Ribatti D, Nico B, Ruggieri S, Tamma R, Simone G and Mangia A. Angiogenesis and antiangiogenesis in triple-negative breast cancer. *Transl Oncol* 2016; 9: 453-457.
- [43] Keenan TE and Tolaney SM. Role of immunotherapy in triple-negative breast cancer. *J Natl Compr Canc Netw* 2020; 18: 479-489.
- [44] Nedeljkovic M and Damjanovic A. Mechanisms of chemotherapy resistance in triple-negative breast cancer-how we can rise to the challenge. *Cells* 2019; 8: 957.
- [45] O'Connor CJ, Chen T, Gonzalez I, Cao D and Peng Y. Cancer stem cells in triple-negative breast cancer: a potential target and prognostic marker. *Biomark Med* 2018; 12: 813-820.